Driven Spatially Autoresonant Stimulated Raman Scattering in the Kinetic Regime

T. Chapman,[1] S. Hüller,[1] P. E. Masson-Laborde,[2] A. Heron,[1] D. Pesme,[1] and W. Rozmus[3]
[1]*Centre de Physique Théorique, CNRS, Ecole Polytechnique, Palaiseau, France*
[2]*CEA, DAM, DIF, F-91297 Arpajon, France*
[3]*Theoretical Physics Institute, Department of Physics, University of Alberta, Edmonton, Alberta, Canada*
(Received 10 October 2011; published 4 April 2012)

The autoresonant behavior of Langmuir waves excited by stimulated Raman scattering (SRS) is clearly identified in particle-in-cell (PIC) simulations in an inhomogeneous plasma. As previously shown via a 3-wave coupling model [T. Chapman *et al.*, Phys. Plasmas **17**, 122317 (2010)], weakly kinetic effects such as trapping can be described via an amplitude-dependent frequency shift that compensates the dephasing of the resonance of SRS due to the inhomogeneity. The autoresonance (AR) leads to phase locking and to growth of the Langmuir wave beyond the spatial amplification expected from Rosenbluth's model in an inhomogeneous profile [M. N. Rosenbluth, Phys. Rev. Lett. **29**, 565 (1972)]. Results from PIC simulations and from a 3-wave coupling code show very good agreement, leading to the conclusion that AR arises even beyond the so-called weakly kinetic regime.

DOI: 10.1103/PhysRevLett.108.145003 PACS numbers: 52.38.Bv, 52.35.Fp, 52.35.Mw, 52.38.Dx

A nonlinear oscillator driven at a swept frequency may undergo autoresonance (AR); under appropriate conditions, the oscillation amplitude may automatically adjust so as to maintain a frequency that is locked to the drive. AR in plasmas has been considered in a variety of contexts, and the exploitation of this phenomenon has a wide range of applications of both fundamental [1,2] and practical interest [3,4]. The impact of AR on scattering processes in plasmas is an area of current research due to the possible role played in inertial confinement fusion (ICF) experiments [5]; in particular, stimulated Raman scattering (SRS) has been identified as the most deleterious of the scattering processes in current ICF experiments using hohlraums [6]. SRS in plasmas is the parametric excitation process in which laser light scatters off of an electron density fluctuation, leading to the growth of both the scattered light and a Langmuir wave (LW) driven by the beating of the laser with the scattered light. The plasma formed near the walls of the hohlraum is steeply inhomogeneous [7], and SRS is expected to be generated in this area, providing conditions conducive to AR. This Letter describes the first clear identification of autoresonance in SRS arising from the kinetic effects of Langmuir waves, and it discusses its importance with regards to the reflectivity.

In inhomogeneous plasmas, the laser wave drives resonantly a spectrum of LW modes. So that AR may be identified unambiguously and studied, we consider initially a single Langmuir wave mode, driven by a pump (the laser wave, propagating in the "forward" direction) and an antiparallel seed (high-intensity scattered light, or a second laser wave, propagating in the "backward" direction). The pump of frequency and wave vector (ω_0, k_0) encounters the seed (ω_1, k_1) in the inhomogeneous plasma. A forward-propagating LW (ω_L, k_L) may be resonantly driven when the matching conditions $\omega_0 = \omega_1 + \omega_L$ and $k_0 = -k_1 + k_L$ are satisfied locally $(\omega_{0,1,L}, k_{0,1,L} > 0)$. The frequencies $\omega_{0,1}$ are chosen such that a LW is resonantly driven at density n_0 in a linear electron plasma density profile $n_e = n_0[1 + (x - x_r)/L]$, where x_r is the linear 3-wave resonance point. L parametrizes the inhomogeneity and can be positive (density increasing in the forward direction, referred to as "positive density gradient") or negative (density decreasing in the forward direction, referred to as "negative density gradient"). While for clarity the density profile discussed here is linear, AR may occur in a broad range of profiles and is subject to remarkably few constraints [8].

In this Letter, we validate by means of particle-in-cell (PIC) simulations that autoresonance in the kinetic regime $k_L\lambda_D \gtrsim 0.25$ [9] can be correctly described [8] by simple mode coupling equations in which the impact of electron trapping on the Langmuir wave evolution is modeled by a nonlinear frequency shift $\delta\omega_{\rm nl}$ (λ_D denotes the usual Debye length). This frequency shift depends on the square root of the Langmuir wave envelope amplitude ε_L such that $\delta\omega_{\rm nl} \propto |\varepsilon_L|^{1/2}$ [10,11]. Thus, starting from resonance and $\varepsilon_L \sim 0$, the growth of ε_L and consequently of $\delta\omega_{\rm nl}$ will detune the 3-wave resonance determined by the fixed laser frequencies $\omega_{0,1}$ [12]. The three waves will undergo an additional shift, this time in wave number, due to the density inhomogeneity while propagating through the plasma. The wave number shift will detune the LW from the ponderomotive drive and, in the absence of nonlinear effects, would saturate the parametric instability. However, the LW may self-adjust ε_L in such a way that the nonlinear component of its frequency $\delta\omega_{\rm nl}(|\varepsilon_L|)$ cancels this shift in wave number, as described in Ref. [8]. This phase locking of the LW to the spatially detuned drive may result in ε_L (and the scattered light) growing well beyond the level

predicted by Rosenbluth [13] in the absence of kinetic effects.

It is sufficient at this stage to write the equation governing the LW evolution under the conditions described previously as the following single wave envelope equation:

$$(\partial_t + c_L\partial_x + ic_L\kappa'(x - x_r) - i\eta|\varepsilon_L|^{1/2})\varepsilon_L = P, \quad (1)$$

where ∂_t and ∂_x represent the partial derivatives of time and space, respectively, κ' parametrizes the spatial wave number detuning such that $\kappa' = \partial_x(k_0 - k_1 - k_L) \approx \omega_{pe}^2(x = x_r)/6Lv_{th}^2k_L$ [14], and c_L is the LW group velocity. ω_{pe} and v_{th} denote the usual electron plasma frequency and the electron thermal temperature, respectively. The parameter η is such that $\delta\omega_{nl}(|\varepsilon_L|) = -\eta|\varepsilon_L|^{1/2}$, with $\eta > 0$ [10]. Using the Poisson equation, the latter relation can be equivalently written as $\delta\omega_{nl}/\omega_L = -\eta_n|\delta n_e/n_0|^{1/2}$, where δn_e denotes the density perturbation amplitude associated with the LW electric field ε_L; η_n is given by $\eta_n \equiv \eta(n_0e/\epsilon_0k_L\omega_L^2)^{1/2}$, where $-e$ is the electron charge. The ponderomotive drive P represents the coupling of the beating electromagnetic waves to the LW.

During AR, the terms $ic_L\kappa'(x - x_r)$ and $i\eta|\varepsilon_L|^{1/2}$ must be approximately equal over an extended region in space, with growth beginning at x_r. This condition implies $c_L\kappa' > 0$, or equivalently $L > 0$. Thus, AR requires a positive density gradient and we expect in this case $|\varepsilon_L| \approx (c_L\kappa'/\eta)^2(x - x_r)^2$, i.e., a parabolic spatial growth of the LW from the point of resonance. The parabolic spatial growth of the LW amplitude in a positive density gradient is one of the key signatures of AR, and should be absent in the negative density gradient cases. Under similar conditions to those adopted in this Letter, Masson-Laborde *et al.* found a good agreement, for the early SRS behavior, between (i) a one-dimensional (1D) 3-wave coupling model using a nonlinear frequency shift similar to ours and (ii) both one-dimensional and two-dimensional (2D) PIC simulations [15]. Thus, the early time SRS behavior can be considered to be determined by 1D effects as long as the Rayleigh length $l_R \sim 5f_\#^2\lambda_0$ is longer than the length l_{AR} of the spatial domain on which AR develops ($f_\#$ and λ_0 denote the optics f number and the laser wavelength, respectively). It will be found further on that for our parameters l_{AR} is in the order of 100–150λ_0, so that our 1D description of the early time behavior is valid for f numbers larger than $f_\# \sim 6$. We therefore consider a 1D problem, noting that AR is possible in higher-dimensional problems [16]. Using the 1D PIC code EMI1D, we studied the growth of the LW driven by counterpropagating electromagnetic (EM) waves in an inhomogeneous plasma. At time $t = 0$, a pump wave [seed wave] is introduced at the left-hand side (lhs) [right-hand side (rhs)] of the simulation window *in vacuo* with intensity $I_{lhs} = 5 \times 10^{15}$ W/cm^2 [$I_{rhs} = 1 \times 10^{13}$ W/cm^2]. The point of resonance x_r is $x_r \equiv 78$ μm, and the other parameters are the laser wavelength $\lambda_0 = 351$ nm, the electron temperature $T_e = 1$ keV, and density $n_0/n_c = 0.05$, n_c denoting the critical density. Across the region in which AR occurs in this example, $k_L\lambda_D$ lies in the range $0.3 < k_L\lambda_D < 0.37$, while for the whole plasma, $k_L\lambda_D$ varies in the range $0.26 < k_L\lambda_D < 0.49$.

In a positive density gradient [$L = +100$ μm, shown in Fig. 1(a)], the driven LW front exhibits a significant spatial growth as it propagates, while the LW amplitude remains approximately constant over the region behind this wave front (we attribute slow growth throughout the plasma to other LW modes). This strong spatial growth is approximately parabolic over the distance $l_{AR} \approx 150\lambda_0$, allowing the LW to reach a significant amplitude after propagating only a short distance from x_r. The black dashed line in Fig. 1(a) plots the LW amplitude expected by assuming the exact cancellation between shifts, $|\varepsilon_L| = (c_L\kappa'/\eta)^2 \times (x - x_r)^2$. Poisson's equation leads then to the density perturbation level $|\delta n_e/n_0| = \alpha(x - x_r)^2$, with $\alpha \equiv (c_L\kappa'/\eta_n\omega_L)^2$. This simple relation predicts with surprising accuracy the maximum instantaneous amplitude of the LW. The values of the parameters in this relation and the apparent offset of the point of initial growth from x_r are discussed later.

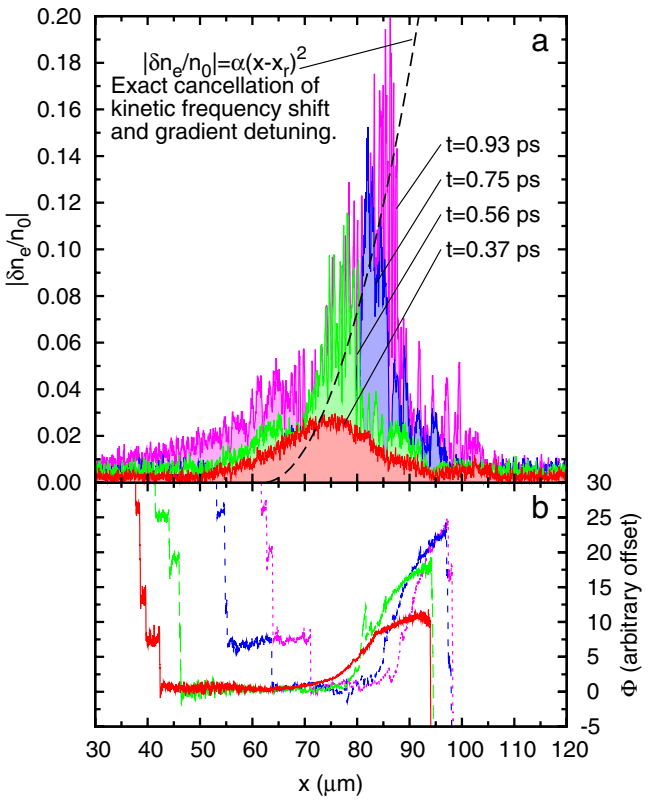

FIG. 1 (color online). (a) Snapshots taken from PIC simulations of the Langmuir wave envelope amplitude, driven by counterpropagating EM waves in a plasma with a positive density profile. (b) The envelope phase mismatch between the EM waves and the Langmuir wave.

We may assign phases ϕ_i to the envelopes of each wave (defined later), relative to an arbitrary fixed value. The difference of phases $\Phi = \phi_0 - \phi_1 - \phi_L$ between the three waves is then an important quantity for identifying AR: if the LW growth is autoresonant, Φ should perform only small oscillations around a constant value [1] over a region in space that lengthens at the speed at which the front propagates. It is this phenomenon of phase locking over a significant spatial extent that allows for the efficient resonant transfer of energy between the three waves. In Fig. 1(b), the phase of the LW is shown at a series of times, exhibiting these key features of spatial AR.

The electron distribution function (EDF) is shown in Fig. 2 in the $\{x, v\}$ phase space, where v denotes the electron velocity. The plateau formed in the EDF at the phase velocity $v_\phi = \omega_L/k_L$ due to trapping is observed to grow in extent and amplitude as a function of x up until the wave front maximum [Fig. 2(a)]. Behind and up to the wave front, the electrons have closed electron trajectories in phase space [Figs. 2(b) and 2(c)]. Beyond the wave front, there is a sharp transition to a mixed phase state [Fig. 2(d)], signaling the sudden end of the AR region in space.

The principal features of the autoresonant LW in PIC simulations may be reproduced using a simple 3-wave model. The total transverse field potential A_z may be written as $A_z = [A_0(x,t)\exp(i\psi_0) + A_1(x,t)\exp(i\psi_1)]/2 +$ c.c., where $A_{0,1}$ are the slowly varying envelopes describing the incident laser and backscattered waves. Similarly, the longitudinal electric field E_x may be written as $E_x = \varepsilon_L(x,t)\exp(i\psi_L)/2 +$ c.c., with $\psi_{0,1,L}(x) = \int_{x_r}^{x} dx' k_{0,1,L}(x') - \omega_{0,1,L}t$.

After substituting $P = \Gamma_L A_0 A_1^*$ into Eq. (1), the following envelope equations for the EM waves make up the 3-wave equations, relevant to the weakly kinetic regime:

$$\mathcal{L}_0 A_0 = -\Gamma_0 A_1 \varepsilon_L, \qquad \mathcal{L}_1 A_1 = \Gamma_1 A_0 \varepsilon_L^*, \tag{2}$$

where $\Gamma_{0,1} = ek_L/4m_e\omega_{0,1}$ and $\Gamma_L = (ek_L/4m_e\omega_L)\omega_{\rm pe}^2$, m_e denoting the electron mass. The waves propagate through the operators $\mathcal{L}_{0,1,L} = \partial_t + c_{0,1,L}\partial_x$, where c_i denotes the group velocity of wave i. The kinetic regime considered here is consistent with the absence of Landau damping to a good approximation.

We solved the 3-wave equations [Eqs. (1) and (2)] using a finite difference method. For simplicity, all parameters except $\Gamma_L = \Gamma_L(x)$ were calculated at x_r and taken to be constant, while the density profile, pump, and seed were unchanged from those defined earlier. The value of η_n, occurring in the relation $\delta\omega_{\rm nl}/\omega_L = -\eta_n|\delta n_e/n_0|^{1/2}$, was found in the PIC simulations to be given by $\eta_n \sim 0.25$ and did not vary greatly with density in the relevant region surrounding x_r. Further details of the model used are given in Ref. [8]. The envelope amplitude of the Langmuir wave is plotted in Fig. 3(a), and the corresponding

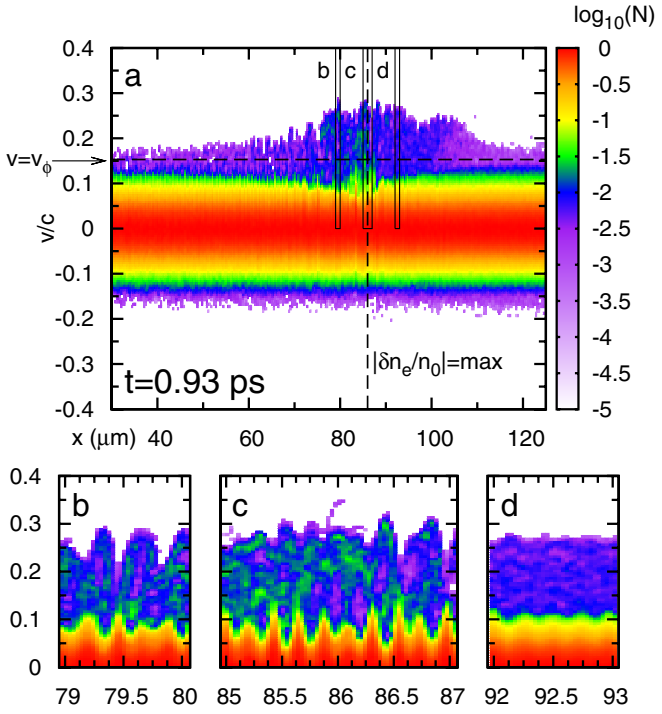

FIG. 2 (color online). The electron distribution function with local normalized particle number N at time $t = 0.93$ ps, calculated from PIC simulations, shown (a) over the entire simulation window and (b)–(d) in detail over selected regions.

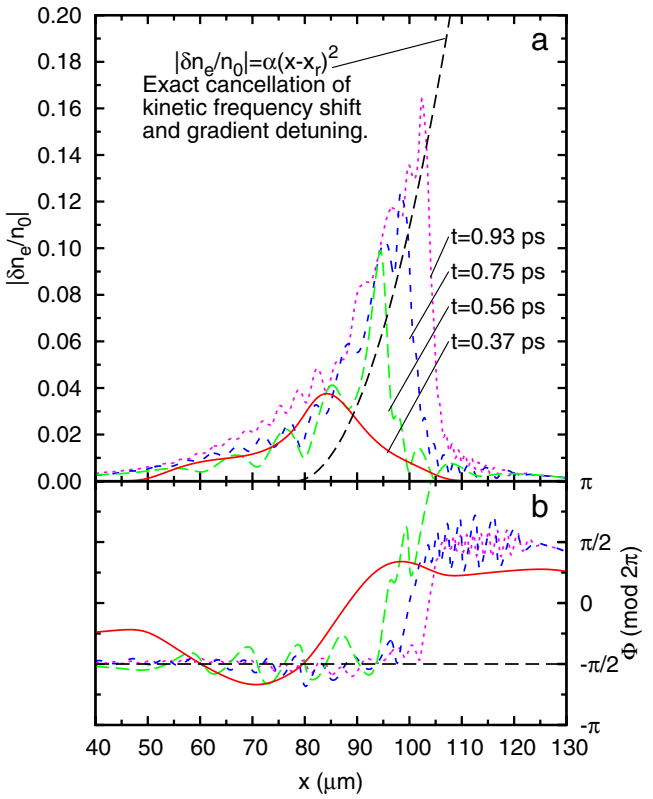

FIG. 3 (color online). As in Fig. 1, but taken from 3-wave simulations. (a) Langmuir wave envelope amplitude. (b) Envelope phase mismatch between the counterpropagating EM waves and the LW.

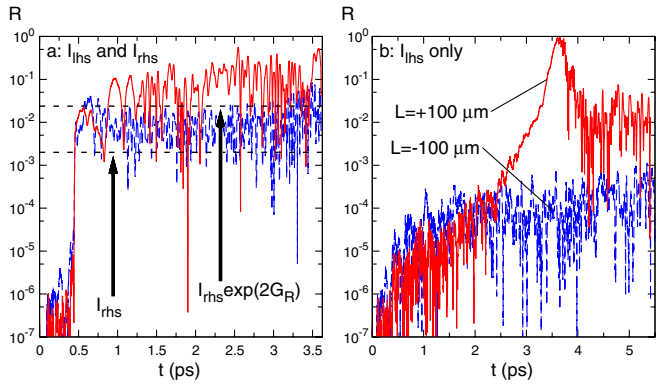

FIG. 4 (color online). Reflectivity taken from PIC simulations when (a) both the lhs laser wave and the rhs seed wave are switched on and (b) only the lhs laser wave is switched on. Results for both positive (red solid line) and negative (blue dashed line) density profiles are shown. Black dashed lines show initial rhs seed level and level expected after Rosenbluth amplification [13].

envelope phase difference $\Phi = \phi_0 - \phi_1 - \phi_L = \arg(A_0) - \arg(A_1) - \arg(\varepsilon_L)$ is plotted in Fig. 3(b). The key features of the PIC simulations are reproduced, with the LW growing along a parabola in space, beginning at the point of initial 3-wave resonance. The time scale over which the autoresonant LW grows is accurately reproduced in 3-wave simulations. Although smaller in size than in the PIC simulation results, there is a similar offset between the observed and predicted initial point of the fitted parabola. In the 3-wave simulations, this is due to the cancellation between shifts not being exact. A mathematical discussion of the mechanism of phase locking is given in Refs. [1,8].

Repeating the simulation shown in Fig. 1 using a negative density profile ($L = -100$ μm) resulted in an initial small growth of the LW at x_r, followed quickly by a decay of the LW. Analysis of the phase mismatch showed no extended region of phase locking. The reflectivity of the plasma for both positive and negative density profiles is shown in Fig. 4 (a). The reflectivity of the plasma is greater by an order of magnitude when the gradient is such that AR may take place. The raised reflectivity of the AR case is maintained even after the autoresonant front ceases to be clearly discernible at around 1.5 ps, and the LW amplitude throughout the plasma remains higher than the negative density profile case until late times (3 ps and beyond). The initial seed wave level $I_{\rm rhs}$ and the reflectivity corresponding to Rosenbluth's prediction in the absence of any saturation mechanism, $I_{\rm rhs}\exp(2G_R)$, are also shown, G_R denoting the Rosenbluth gain factor defined in Ref. [13]. The AR case exhibits a reflectivity above this level, while the case where AR is not possible exhibits a reflectivity below it.

The spatial extent of AR (and thus the maximum LW amplitude attained via AR) may be limited due to a number of causes: (1) damping of the LW, (2) wave breaking, (3) the vanishing of the value of k_L as the LW propagates to higher densities, or (4) a loss of phase locking due to the growth of the LW, as described in Ref. [8]. In the autoresonant case (Fig. 1), increasing the intensity of the lhs (or rhs) EM wave by a factor of 2 increased the amplitude at which the autoresonant Langmuir wave saturated by a factor of $\sim$1.2. If the AR was limited purely by cause (4), this factor would be closer to $\sim$4 [8], while cause (3) may also be ruled out. It is thus likely that the loss of autoresonance here is due to a combination of factors, such as damping and the onset of wave breaking.

In the preceding case, AR of a single LW mode was unambiguously observed by imposing a narrow band EM seed at the rhs boundary. We now consider the plasma reflectivity in the realistic case where the backscattered wave amplitude is seeded, together with the LW, at all points in the plasma with a broadband noise describing the electron density fluctuations (i.e., $I_{\rm rhs} = 0$). Even more than in the previous narrow band case, the SRS reflectivity is observed to be higher when the gradient is positive compared to when it is negative (for the parameters used in this Letter, this increase is a factor of 1×10^4 at the first saturation of the reflectivity, and tends towards a factor of $\sim$15 [Fig. 4(b)]). We have clearly observed this effect for values of L and $k_L\lambda_D$ in the ranges $1800 < k_0 L < 9000$ and $0.3 < k_L\lambda_D < 0.37$ (evaluated at n_0). Thus, AR destabilizes the Rosenbluth solution [13], leading to a strong enhancement of the SRS reflectivity. This enhancement persists beyond the first saturation of the SRS reflectivity, and is important beyond the regime usually deemed "weakly kinetic."

On the basis of the results obtained in Ref. [15], it may be estimated that our 1D results correctly describe the multidimensional physics for times shorter than $\sim$2.4 ps for the plasma parameters considered in this Letter. More generally, one may assume that the initial nonlinear evolution of SRS is very well described by 1D modeling until the LW transverse modulations become dominant. During this initial phase, autoresonance could play a decisive role in the LW evolution, and consequently on the long-term 2D nonlinear SRS behavior. An amplifier scheme to transfer beam energy via SRS in inhomogeneous plasmas has been suggested in Ref. [17], for which, based on the results presented here, AR in the kinetic regime may prove to be a positive application.

We gratefully acknowledge the support of the Gaspard Monge scholarship program of Ecole Polytechnique and of the Agence Nationale de Recherche (project "CORPARIN," ANR-07-BLAN-0004). Simulations have been performed using resources from GENCI-IDRIS.

[1] L. Friedland, Phys. Rev. E **55**, 1929 (1997).
[2] P. Khain and L. Friedland, Phys. Plasmas **17**, 102308 (2010).

[3] G. B. Andresen *et al.*, Phys. Rev. Lett. **106**, 025002 (2011).
[4] V. V. Gorgadze, L. Friedland, and J. S. Wurtele, Phys. Plasmas **14**, 082317 (2007).
[5] E. A. Williams *et al.*, Phys. Plasmas **11**, 231 (2004).
[6] S. H. Glenzer *et al.*, Science **327**, 1228 (2010).
[7] D. Hinkel *et al.*, Phys. Plasmas **18**, 056312 (2011).
[8] T. Chapman *et al.*, Phys. Plasmas **17**, 122317 (2010).
[9] J. L. Kline *et al.*, Phys. Rev. Lett. **94**, 175003 (2005); J. L. Kline *et al.*, Phys. Plasmas **13**, 055906 (2006).
[10] G. J. Morales and T. M. O'Neil, Phys. Rev. Lett. **28**, 417 (1972).
[11] R. L. Dewar and W. L. Kruer, Phys. Rev. Lett. **28**, 215 (1972).
[12] H. X. Vu, D. F. DuBois, and B. Bezzerides, Phys. Rev. Lett. **86**, 4306 (2001).
[13] M. N. Rosenbluth, Phys. Rev. Lett. **29**, 565 (1972).
[14] C. S. Liu, M. N. Rosenbluth, and R. B. White, Phys. Rev. Lett. **31**, 697 (1973).
[15] P. E. Masson-Laborde *et al.*, Phys. Plasmas **17**, 092704 (2010).
[16] O. Yaakobi and L. Friedland, Phys. Plasmas **15**, 102104 (2008).
[17] V. M. Malkin, G. Shvets, and N. J. Fisch, Phys. Rev. Lett. **84**, 1208 (2000).